ATMOSPHERIC RESEARCH

RECHERCHE ATMOSPHÉRIQUE

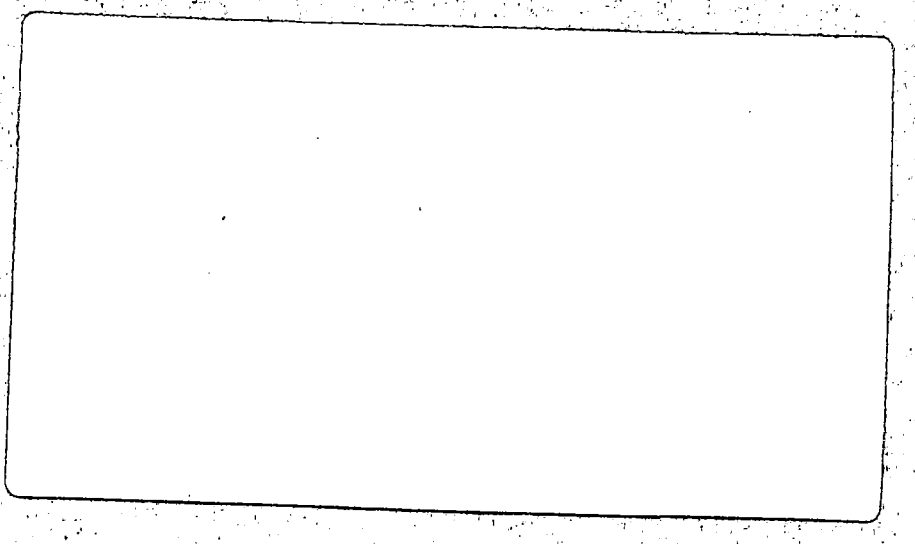

ATMOSPHERIC ENVIRONMENT

ENVIRONNEMENT ATMOSPHÉRIQUE

Report - ARQL - 76/2

Application of Acoustic Sounding to Estimating Diffusion in an Atmospheric Boundary Layer

Bryan R. Kerman,
Boundary Layer Research Division,
Air Quality and Inter-Environmental Research Branch
Downsview, Canada.

Abstract

An acoustic sounder system can be configured to provide estimates of the vertical profile of velocity and the dissipation rates of kinetic and potential energy. A method based on the concepts of boundary-layer similarity theory is outlined by which the characteristic velocity in a freely convective boundary layer is deduced from the inversion height and a combination of any two of the mean wind in the layer, the dissipation rate of turbulent kinetic energy, and that of turbulent potential energy near the inversion. These values, in conjunction with the mean velocity, are used to establish the normalized heights, downwind and cross-wind distances, and cross-wind integrated concentrations. The normalized lateral and vertical standard deviations are then deduced from empirically established laboratory relationships for nonbuoyant particulates. Preliminary analysis indicates a similar methodology may be applicable to the stable boundary layer.

1. Introduction

The same atmospheric process that scrambles acoustic waves diffuses pollutants. Therefore, it is natural that measurements of acoustic scattering near the ground should be directly applicable to estimating the diffusion of passive contaminants introduced into the planetary boundary layer. In this paper a method is proposed for utilizing the variables directly sensed by a bistatic Doppler equipped acoustic sounding system for estimating some of the statistical properties of the downwind concentration field. The analysis will be limited to a discussion of the estimation of the concentration field in a freely convective boundary layer, because of the current status of experimental results. However, as will be seen, the method appears to have a somewhat broader applicability.

Original efforts at implementing acoustic echo sounding in air pollution related studies primarily used the height of the lowest inversion as a principal controlling variable (see for example, Beran and Hall, 1974) and the classification of the scattering pattern relative to thermal stability (Russell et al., 1974). This methodology was followed by preliminary analyses of the thermal stability structure in terms of boundary layer similarity (Brown et al., 1975; Kerman, 1976) using directly measured values of the scattering, the so-called velocity and thermal structure 'constants' C_v^2 and C_T^2 where

$$C_v^2 = \alpha\ \varepsilon^{2/3}$$

and

$$C_T^2 = \beta\ \chi\varepsilon^{-1/3}$$

where ε and χ are the destruction rates of turbulent kinetic and potential energy and the coefficients α and β, are universal constants for a turbulent flow with a sufficiently large Reynolds number. Measurements of C_v^2 and C_T^2 are being discussed at this session and will not be reviewed here.

The meteorological analysis technique of this paper is a particularization of the methods of Brown and Kerman for a distinct stability regime, the so-called free convection regime. However, the thrust here is towards a fuller coordination of the results of free convection theory and measured values of C_v^2, C_T^2, the inversion height, h, and wind speed $\overline{U}$, with the estimation of the statistics of concentrations of non-buoyant pollutants. Next, some of the theoretical and experimental results of a freely convective atmospheric boundary layer are reviewed.

2. Structure of a Freely Convective Atmospheric Boundary Layer

In considering a steady, horizontally homogeneous planetary boundary layer, it is assumed that the vertical structure of mean and turbulent parameters can be reduced to similar form with the use of an appropriate scaling length, velocity and temperature. A boundary layer which has its dynamics dominated by a large upward surface heat flux $g/T\ Q_o$, and an upper stable layer with a base at a height, h, has certain natural velocity, time, and temperature scales associated with it, which are

$$w_* = \left(g/T\ Q_o\ h\right)^{1/3}$$

$$t_* = h/w_*$$

$$\theta_* = \left(\frac{Q_o^2}{g/T\ h}\right)^{1/3}$$

However, in the presence of a non-zero wind velocity through the boundary layer, it is necessary to consider a possible modification of the basic control mechanism by the downward flux of momentum linking the outer geostrophic layer to the surface. This introduces another set of characteristics for velocity and time

$$u_* = \left(-\overline{uw}\right)_{z_o}^{1/2}$$

$$t_*' = f^{-1}$$

where f is the Coriolis parameter associated with geostrophic flow and z_o is the

surface roughness height. Tennekes (1970) argues that there exists a region of free convection where

$$\frac{hf}{w_*} << 1$$

such that the buoyant eddies are sufficiently detuned from the mechanical eddies that there is an insignificant momentum transfer, i.e.,

$$\frac{u_*}{w_*} << 1$$

Wyngaard, Arya and Cote (1974) argue that there exists an alternative mechanism for comparable time scales for energy and momentum transfer involving a self-adjusting process to the mean velocity field to minimize the shear and the momentum transfer. In any case the ratio, u_*/w_*, represents the relative rates of mechanical and buoyant energy generation in a convective regime.

Some results of a recent field experiment (Kaimal et al., 1976) are displayed in Figs. 1 to 3 as examples of the apparent similarity of some turbulent parameters in a convective boundary layer.

Figs. 1 and 2 show the variation of the vertical velocity variance and the energy containing scale with height up to the inversion. If one defines an eddy diffusivity in terms of these values given by

$$K \sim \overline{w^2}^{1/2} \lambda_m$$

as is often done, it is implied that K also increases monotonically up to h. Accordingly the eddy diffusivity does not have the local maximum within the layer and the zero diffusivity near h often utilized in modelling the boundary layer. This result should be kept in mind in the later discussion of measured concentration profiles with height.

Fig. 3 shows the structure of ε, normalized by the surface heat flux, $g/T Q_o$. As can be seen, within the limits of the logarithmic coordinates, ε approaches a fixed ratio of the surface heat flux. This result is even more apparent in terms of unscaled variables as demonstrated by Kaimal et al. In order to see

some reason for this result, it is necessary to consider the local balance of the production of kinetic energy with height. Results of Lenschow (1974) (Fig. 4) indicate that at a height of about 0.1 h the vertical heat flux decreases linearily with height, the convergence of the vertical flux of kinetic energy increases linearily with height, the shear contribution is negligible and the dissipation rate is approximately constant with height. Lenschow states, that within the limits of his instrumentation, the kinetic energy balance is

$$\varepsilon = \frac{g}{T}\,\overline{w\theta} - \frac{\partial}{\partial z}\,\overline{we^2}$$

ε is essentially a local residual between the production term $g/T\ \overline{w\theta}$ and the vertical energy flux convergence term, which is a loss near the ground, up to about 0.5 h and a gain above. In order to examine this balance further, we represent the dissipation in a Taylor series about h,

$$\varepsilon = \varepsilon_h + \left.\frac{\partial \varepsilon}{\partial z}\right|_h (z-h) + \left.\frac{\partial^2 \varepsilon}{\partial z^2}\right|_h \frac{(z-h)^2}{2} + \ldots$$

and the heat and energy fluxes as Taylor series about $z = z_o$, the surface roughness length.

$$\overline{w\theta} = \left.\overline{w\theta}\right|_{z_o} + \left.\frac{\partial \overline{w\theta}}{\partial z}\right|_{z_o} z + \left.\frac{\partial^2 \overline{w\theta}}{\partial z^2}\right|_{z_o} \frac{z^2}{2} +$$

$$\overline{we^2} = \left.\frac{\partial \overline{we^2}}{\partial z}\right|_{z_o} z + \left.\frac{\partial^2 \overline{we^2}}{\partial z^2}\right|_{z_o} \frac{z^2}{2} +$$

where $\left.\overline{we^2}\right|_{z_o} = 0$ necessarily at a solid surface.

From the basic balance implied by the kinetic energy equation and the respective Taylor series

$$\varepsilon_h + \left.\frac{\partial \varepsilon}{\partial z}\right|_h h + \ldots = \left.\frac{g}{T}\overline{w\theta}\right|_{z_o} - \left.\frac{\partial}{\partial z}\overline{we^2}\right|_{z_o}$$

and $$\left.\frac{\partial \varepsilon}{\partial z}\right|_h + \left.\frac{\partial^2 \varepsilon}{\partial z^2}\right|_h h \ldots = \frac{\partial}{\partial z}\left(\frac{g}{T}\overline{w\theta} - \frac{\partial}{\partial z}\overline{we^2}\right)_{z_o}$$

In the first of these results, using the observation that there is an insignificant variation of ε when weighted by the depth of the inversion, the dissipation rate in the outer boundary layer can be described in terms of the production-loss imbalance near the surface. Additionally the lack of variation in ε with height, ignored in the first equation, is itself associated with a lack of variation in the fluxes of heat and energy flux near the ground. That is, the same relationship of time scales that defines the characteristics of the surface constant flux layer (Lumley and Panofsky, 1964, p 99) also controls the constancy of ε near the inversion.

The point of analysing the asymptotic behaviour of ε near h is simple. If such a behaviour is dynamically realistic and if such a vertical structure is not too sensitive to the constraint of the boundary layer being in a steady state, the asymptotic value of ε, denoted ε_h, represents a basic boundary layer variable. As such it shares an equally important place with classical normalizing variables such as u_*, w_* and T_* in a similarity analysis. Of added significance to the field of acoustic sounding it is a directly measured variable. Additionally, it is suggested that any structure that is observed in the outer boundary layer intuitively represents an areal weighting of surface effects. Therefore, where it is difficult to estimate a realistic surface stress or heat flux in a region of mixed surface roughness and heat capacity, values such as ε_h, necessarily represent naturally horizontally-averaged parameters.

As a demonstration of these remarks, consider an alternative scaling of the freely convective boundary layer in terms of ε_h and h. The characteristic velocity is

$$V_h = (\varepsilon_h \, h)^{1/3}$$

and the characteristic temperature

$$\theta_h = \varepsilon_h / \left(\frac{g}{T} V_h\right) = \varepsilon_h^{2/3} / \left(\frac{g}{T} h^{1/3}\right)$$

The ratio of V_h and w_*

$$\frac{V_h}{w_*} = \left(\frac{\varepsilon_h}{g/T \, Q_o}\right)^{1/3}$$

is implied to be a constant ($\sim$ 0.89) in the observations of Kaimal et al. so that V_h and w_* are interchangable. Fig. 5 demonstrates the similarity form of $\overline{w^2}/V_h^2$ with height. Apparently V_h reduces the Minnesota data to similarity form equally well as the original w_* scaling.

However, rather than have two sets of similarity functions which are more or less equivalent it is more reasonable to simply derive $g/T \, Q_o$ and w_* in terms of ε_h and V_h given measurements of h and ε_h. The question that arises next is to what accuracy such a reduction is possible. In addition to the sampling problem associated with the wide dynamic range of the acoustic sounder system, there is a problem in accounting for the experimental scatter with non-ideal meteorological conditions. Towards this latter problem, let us consider the scatter in the relationship $\varepsilon_h / \left(g/T \, Q_o\right)$ drawn from the Minnesota experiment more closely. The most likely cause of the experimental scatter arises from differing shear production rates which should scale with u_*/w_*. In Fig. 6 $\varepsilon_h / \left(g/T \, Q_o\right)$ is examined as a function of u_*/w_*. Apparently the ratio of dissipation aloft and surface heat flux monotonically decreases with increasing shear production. One would not have expected this result intuitively. Apparently, the increased inversion height with shearing must also be considered. The circled points in Fig. 6 represent late afternoon transition cases when the assumption of a steady, free convective state may not be valid.

Apparently if $g/T\ Q_o$ is to be accurately estimated from ε_h we require prior knowledge of u_*/w_*. Such information is available from the second variable measured by the acoustic sounder, namely C_T^2, or $\chi\varepsilon^{-1/3}$. Free convection theory predicts that

$$C_T^2 \sim Q_o^{4/3} \left(g/T\right)^{-2/3} z^{-4/3}$$

a result which is well supported by the Minnesota data (Fig. 7). Obviously if a new parameter, ζ, is formed by substitution of ε_h for $g/T\ Q_o$ in the above equation, it must necessarily carry a u_*/w_* variation. We define accordingly

$$\zeta = \beta^{-1} \left(g/T\ C_T^2\right) \left(z\ \varepsilon_h^{-1}\right)^{4/3}$$

where $\beta = C_T^2/\left(\chi\varepsilon^{-1/3}\right) \simeq 3.2$

Fig. 8 shows the variation of $\varepsilon_h/\left(g/T\ Q_o\right)$ with ζ, which is similar to its variation with u_*/w_*. Accordingly it is possible from Fig. 8 to more accurately estimate $g/T\ Q_o$ from ε_h using the parameter ζ. Additionally having $g/T\ Q_o$ (and h) and so w_*, it is possible to also estimate u_* from the interrelationship of u_*/w_* to ζ.

Alternatively w_* (or u_*) could be estimated from the nearly constant mean wind velocity, $\bar{U}_h$, in the convective boundary layer. Fig. 9 demonstrates the similarity of $\bar{U}_h/w_*$ to the parameter ζ. A corresponding organized structure would be expected to hold for $\bar{U}_h/u_*$ in terms of ζ. If both ε_h and $\bar{U}_h$ are available from a Doppler bistatic acoustic sounder system, then there exists several ways to estimate the surface heat flux and stress from measurements made in the outer boundary layer.

In summary, there exists an organized structure in terms of C_v^2, C_T^2 and $\bar{U}$ in free convection, which can be measured by an acoustic sounder, and which can be utilized either to define an alternative form of free convection boundary layer similarity or to derive the scaling variable of the classical theory. The latter method is preferred at this time as it allows immediate application with some well-known results of diffusion in a convective boundary layer.

3. Diffusion in a Freely Convective Boundary Layer

Deardorff and Willis (1975) have described a water tank experiment in which they have attempted to simulate the diffusion of non-buoyant, chemically inert pollutants within the atmosphere's convective boundary layer. Their results are exceptional in their completeness. Deardorff and Willis have extended free convection similarity to the diffusion variables. Time after release, t, has been normalized

$$\hat{t} = (w_*/h)t$$

(essentially the number of large eddy turnovers), the lateral distance, y, and the vertical height, z, by

$$\hat{y} = y/h \qquad \hat{z} = z/h \quad ,$$

and the horizontal distance downstream from the release point, x, by

$$\hat{x} = x/(\bar{U}h/w_*)$$

The concentration, c, arising from a continuous point, at a rate, s, is normalized by

$$\hat{c} = (h^2 \bar{U}/s)\, c$$

The standard deviations in the lateral and vertical dimensions are also normalized by h, i.e.

$$\hat{\sigma}_y = \sigma_y/h$$

and

$$\hat{\sigma}_z = \sigma_z/h$$

The lateral spreading both in the water tank and the atmosphere (Pasquill, p 227) has been observed to be Gaussian and describable by a form

$$\hat{c}\ (\hat{x},\ \hat{y},\ \hat{z}) = \frac{\overline{\hat{c}}^{\,y}\ (\hat{x},\ \hat{z})}{(2\pi)^{1/2}\ \hat{\sigma}_y} \exp\ (-\hat{y}^2/2\hat{\sigma}_y^{\,2})$$

where

$$\overline{\hat{c}}^{\,y} = \int_{-\infty}^{\infty} \hat{c}\ (\hat{x},\ \hat{y},\ \hat{z})\ d\hat{y}$$

is the cross-wind integrated concentration. Deardorff and Willis have shown that $\hat{\sigma}_y$ is adequately described by

$$\hat{\sigma}_y = \left[0.26\ \hat{x}^2/(1 + 0.91\ \hat{x})\right]^{\frac{1}{2}}$$

which agrees with the theoretical limits

$$\hat{\sigma}_y \to \hat{x} \qquad \hat{x} << 1$$

and

$$\hat{\sigma}_y \to \hat{x}^{3/2} \qquad \hat{x} >> 1$$

The cross-wind integrated concentration $\overline{\hat{c}}^{\,y}$ as tabulated by Deardorff and Willis and reproduced in Fig. 10 shows an interesting maximum concentration centered near $\hat{z} \approx 0.8$ and $\hat{x} \approx 1.5$. This maximum indicates that the pollutants released near the surface are swept up into the upper reaches of the boundary layer - within 1 to 2 turnovers of the large energy containing eddies. Such a maximum could not be predicted on the basis of a scalar eddy diffusivity relationship because there had to have been a counter-gradient transfer by the convective plumes to establish the elevated maximum.

The results of Deardorff and Willis for the vertical spreading have been fitted for a Gaussian plume formulation although it is not clear, based on the results of Lamb, Chen and Seinfeld (1975) and Pasquill and Smith (1974) that such a model is appropriate. Their parameterization is a complicated function of $\hat{x}$, u_*/w_*, and the normalized release height, $\hat{z}_s = z_s/h$, and will not be reproduced here. Suffice it to say that their results approach the theoretical limits

$$\sigma_z \rightarrow u_* t \qquad (\hat{z}_s \ll 1 \ , \ w_*/u_* \ll 1)$$

and

$$\sigma_z \rightarrow \hat{x}^{3/2} \qquad (\hat{x} \gg 1 \ , \ \hat{z}_s \ll 1)$$

It has been carefully pointed out by Deardorff and Willis that these results can only be generalized so far. It is recognized that mesoscale meandering cannot be included in a non-rotational tank of fixed dimensions. The results apply only for a fixed release height; they assume a single point release of a neutrally buoyant, inert contaminant and they require the boundary layer to be sufficiently well-developed convectively. Also, the Gaussian assumption is recognized as not being a good approximation for the vertical spreading for $\hat{x} > 0.5$. Clearly these limitations can be approached singly and an extended parameterization is possible.

It is interesting to compare the water tank results and parameterization with atmospheric experiments. Willis and Deardorff (1976) have done an intercomparison with some results of Islitzer (1961) and Islitzer and Dumbauld (1973). A summary of the respective results is given in Fig. 11. The results of Islitzer (1961) refer to downstream distances of 150 to 1800 m, an elevated release point, $\hat{z}_s \simeq .023$, whereas those of Islitzer and Dumbauld extend to 3200 m and a surface release point. As shown, the water tank tends to slightly overestimate the short range atmospheric results. As pointed out by Willis and Deardorff, this may be due to the atmospheric boundary layer having not been fully convective, or the atmospheric variances having been excessively filtered.

There has been no attempt to validate the existence of the elevated maximum concentration in the atmosphere. However, there are reports Edinger, 1973) of locally large oxidant concentrations at the base of and in thin layers within an inversion over Los Angeles. A direct comparison with the laboratory results is not warranted because of the areal source nature of the situation and the influence of mountains downstream. Another diffusion experiment (Crabbe, 1976) in a convective regime was analysed and the results are presented in Table 1.

Table 1

(Units MKS)

Experiment	u_*	w_*	h	L	$\bar{U}_h$	$\hat{x}$	$\hat{z}$	$\bar{\hat{c}}^y$
1	.45	2.4	790	- 15	6	15	.038	.033
							.190	.030
							.670	.021
3	.49	1.2	1400	-520	11	2.3	0.64	.371
							.393	.281
							.893	.096

In Crabbe's Experiment 1, a free convection regime appears to be approached ($u_*/w_* = .19$; $\bar{U}_h/w_* = 2.5$) but comparison with the water tank results is not possible ($\hat{x} = 15$) except to note that the assumption of uniform mixing far downstream seems to be borne out. In Experiment 3, a free convection regime definitely does not exist ($u_*/w_* = .49$; $\bar{U}_h/w_* = 9.2$) although the normalized downstream distance ($\hat{x} = 2.3$) is within the laboratory range. The vertical distribution of $\bar{\hat{c}}^y$ in this case of forced convertion differs significantly from the laboratory results at the same value of $\hat{x}$. These inclusive results, if nothing else, indicate some of the difficulties that will be encountered in staging controlled diffusion experiments to validate the results of Deardorff and Willis.

4. Extension to Other Stability Regimes

In Section 2 it was pointed out that the gradient of ϵ near the base of the inversion was controlled by the gradients of certain fluxes near the surface. This may sound like a contradiction to refer to significant gradients in the so-called constant flux layer, but this is not really the case. The constant flux layer (Blackadar and Tennekes, 1968) refers to a depth large compared to the rough elements. If an alternative scaling by the depth of the entire mixed layer is employed, the largest gradients in the new coordinate system will occur near the surface. Accordingly when discussing depth comparable to the mixing layer height itself, it is reasonable to find a relationship between the rate of destruction of turbulent kinetic energy in the outer boundary layer and the gradients of production near the surface.

The obvious question to ask is whether such a relationship could be expected to hold for other steady state situations with different stratifications. To study this question we draw heavily on some experimental results from a tall tower. Fig. 12 is a replotting of the unstable results of Volkovitskaya and Ivanov (1970) using the Minnesota relationships discussed in Section 2 to estimate w_* and h. The scatter is somewhat larger than in these authors' original paper but not incompatible with the Minnesota experiment. Most of the scatter seems to be associated with the rescaling itself as many individual runs indicate the asymptotic structure in ϵ. Another illustration drawn from Volkovitskaya and Ivanov's work, for neutral stratification, is presented in Fig. 13. The scaling for this figure is based on a new scaling length, z_h, defined by the apparent constant value of ϵ aloft, denoted ϵ_h, seen in individual runs and the only significant velocity for neutral stratification, u_*. z_h is given by $z_h = u_*^3/\epsilon_h$. Intuitively the length, z_h, corresponds to a region of overlap of the scaling influence of ϵ_h and u_* which will be near a height where the gradient of surface fluxes becomes insignificant. This premise is borne out in Fig. 13 as there is no perceivable trend to ϵ/ϵ_h above $z \sim z_h$. The stable tower results as normalized by Volkovitskaya and Ivanov utilizing u_* as a characteristic velocity and $\kappa\, u_*\, f^{-1}$ as a scaling length also imply a potentially constant value of ϵ aloft. Their results are not reproduced here because they do not scale by a more obvious choice length choice, L, the Monin-Oboukov length where

$$L = \frac{-u_*^3}{\kappa\, g/T\, Q_o}$$

On the basis of the Kansas experiment results (Wyngaard and Cote, 1971), ε appears also to approach a constant for sufficiently large values of z/L. Wyngaard and Cote results imply

$$\varepsilon \simeq 2.5 \frac{u_*^3}{xz} \left(\frac{z}{L}\right)^{0.9}$$

for $z/L > 0.4$ approximately, which varies only weakly in z. However, their results are limited to $z/L \lesssim 0.6$ so that there is no direct confirmation of the apparent asymptotic structure of ε. There is evidence from the companion paper of Businger et al. (1971) that the shear in a stable region scales as u_*/L up to $z/L > 1$. Therefore, we tentatively conclude that ε will appear to be constant at heights comparable to L, and will scale as u_*/L or equivalently $g/T\, Q_o$. Notwithstanding the analysis of Volkovitskaya and Ivanov, there is no evidence presently to support extending our conclusion, say to a height range, $z/L \sim 10$.

5. Summary

There exists a natural linkage between variables, C_v^2, C_T^2, h and $\bar{U}_h$, measured by an acoustic sounder, the structure of the freely convective boundary layer and the diffusion from a nearground source. A method has been presented for utilizing these variables to imply the areally averaged surface heat and momentum fluxes which in turn can be used to estimate certain statistics of the downwind concentration field.

Certain steps in the development need future consideration. The entire question of experimental accuracy in determining C_v^2 and C_T^2 needs to be studied. There is a need for additional boundary layer data to corroborate the Minnesota data set. There is also an obvious requirement to conduct a controlled atmospheric diffusion study to validate the results of the laboratory results of Deardorff and Willis. Finally, more and better data are required in order to quantify the structure of C_v^2 and C_T^2 aloft and to relate it to a dynamical framework in other stability regimes.

6. References

Beran, D.W. and F.F. Hall, Jr., 1974: Remote sensing for air pollution meteorology. *Bull. Amer. Met. Soc., 55* 1097-1105.

Blackadar, A.K. and H. Tennekes, 1968: Asymptotic similarity in neutral barotropic planetary boundary layers. *J. Atmos. Sci., 25,* 1015-1020.

Brown, E.H., D.W. Beran, A.S. Frisch and C.G. Little, 1975: Measuring atmospheric critical parameters by echosondes. Paper presented at the Third Workshop in Atmospheric Acoustics, Toronto, Canada.

Businger, J.A., J.C. Wyngaard, Y. Izumi and E.F. Bradley, 1971: Flux-profile relationships in the atmospheric surface layer. *J. Atmos. Sci., 28,* 181-189.

Crabbe, R.S., 1976: Examination of gradient-transfer theory for vertical diffusion over mesoscale distances using instrumented aircraft. Report LRT-UA-37, National Research Council of Canada, 33 pp.

Deardorff, J.W. and G.E. Willis, 1975: A parameterization of diffusion into the mixed layer. *J. Applied Met., 14,* 1451-1458.

Edinger, J.G., 1973: Vertical distribution of photochemical smog in Los Angeles basin. *Environ. Sci. and Tech., 7,* 247-252.

Islitzer, N.F., 1961: Short-range atmospheric dispersion measurements from an elevated source. *J. Met., 18,* 443-450.

Islitzer, N.F. and R.K. Dumbauld, 1963: Atmospheric diffusion-deposition studies over flat terrain. *Int. J. Air and Water Poll. 7,* 999-1022.

Kaimal, J.C., J.C. Wyngaard, D.A. Haugen, O.R. Cote, Y. Izumi, J.S. Caughey and C.J. Readings, 1976: Turbulence structure in the convective boundary layer. *Q. J. Roy. Met. Soc.,* to appear.

Kerman, B.R., 1976: A note on the interpretation of acoustic sounder returns. *Boundary-Layer Met.,* to appear.

Lamb, R.G., W.H. Chen and J.H. Seinfeld, 1974: Numerico-empirical analysis of atmospheric diffusion theories. *J. Atmos. Sci., 32,* 1794-1807.

Lenschow, D.H., 1974: Model of the height variation of the turbulent kinetic energy budget in the unstable planetary boundary layer. *J. Atmos. Sci., 31,* 465-474.

Lumley, J.L. and H.A. Panofsky, 1964: 'The Structure of Atmospheric Turbulence'. Interscience, p 99.

Pasquill, F., 1974: 'Atmospheric Diffusion.' Wiley, p 227.

Pasquill, F. and F.B. Smith, 1970: The physical and meteorological basis for the estimation of the dispersion of windborne material. Proc. Second Intern. Air Poll. Conf., New York, Academic Press.

Russell, P.B., E.E. Utha and F.L. Ludwig, 1974: A comparison of atmospheric structure as observed with monostatic acoustic sounder and lidar techniques. *J. Geophys. Res., 79,* 5555-5566.

Tennekes, H., 1973: A model for the dynamics of the inversion above a convective boundary layer. *J. Atmos. Sci., 30,* 558-567.

Volkovitskaya, Z.I. and V.N. Ivanov, 1970: Turbulent energy dissipation in the atmospheric boundary layer. *Atmos. and Oceanic Phys., 5,* 249-254.

Willis, G.E. and J.W. Deardorff, 1976: A laboratory model of diffusion into the convective planetary boundary layer. *Q. J. Roy. Met. Soc., 102,* 427-445.

Wyngaard, J.C., S.P.S. Arya and O.R. Cote, 1974: Some aspects of the structure of the convective planetary boundary layer. *J. Atmos. Sci., 31,* 747-754.

Wyngaard, J.C. and O.R. Cote, 1971: The budgets of turbulent kinetic energy and temperature variance in the atmospheric surface layer. *J. Atmos. Sci., 28,* 190-201.

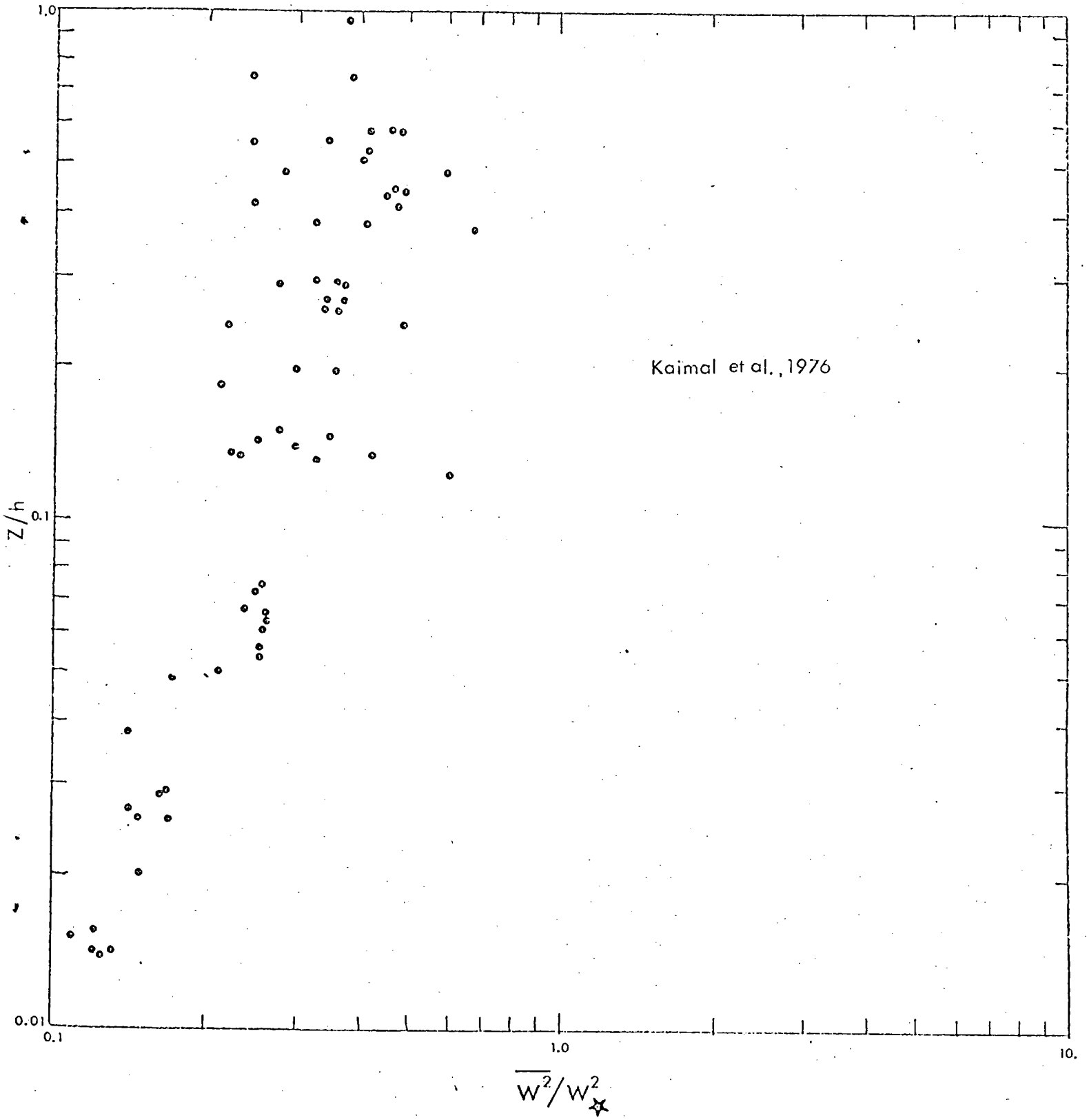

Figure 1

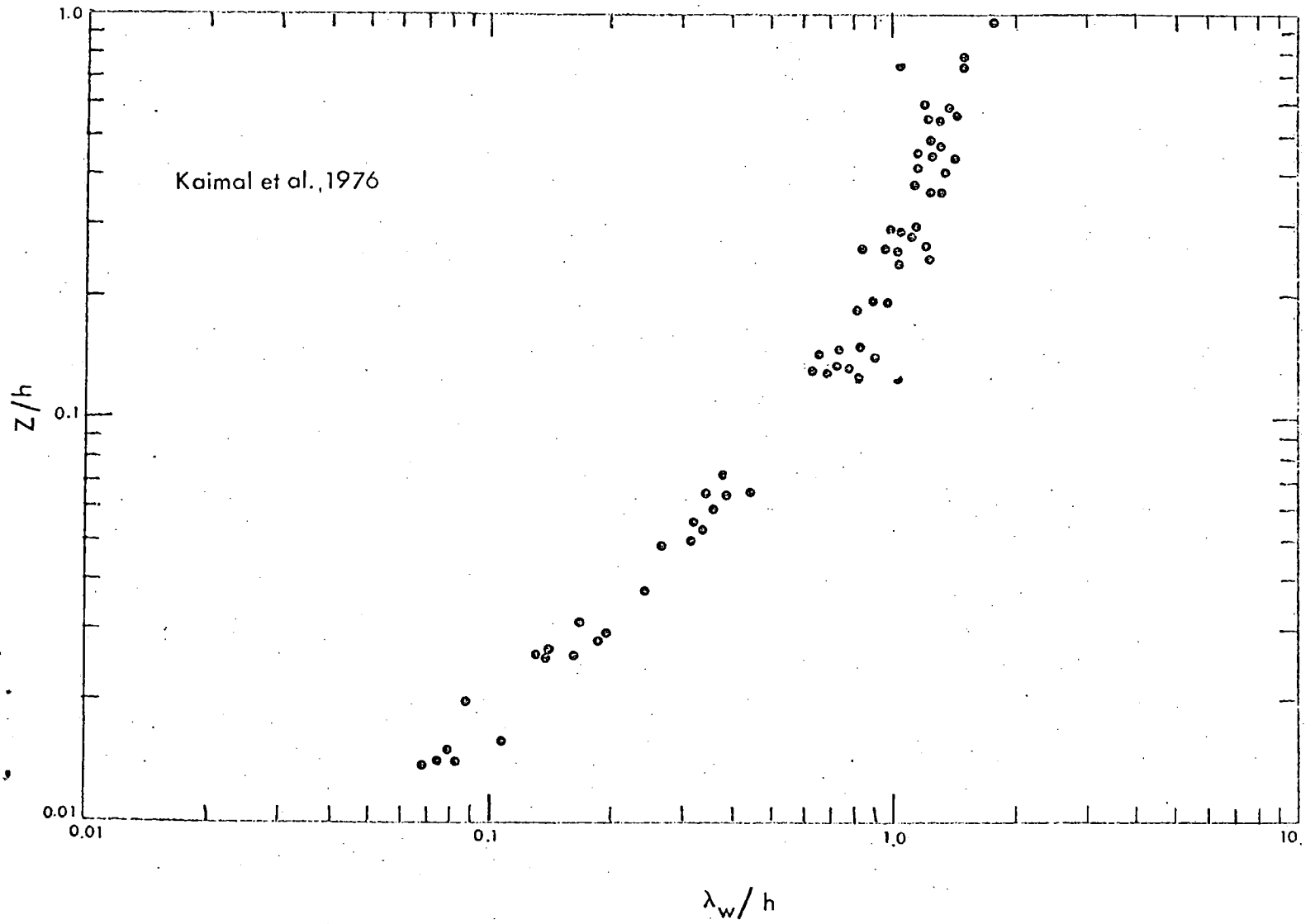

Figure 2

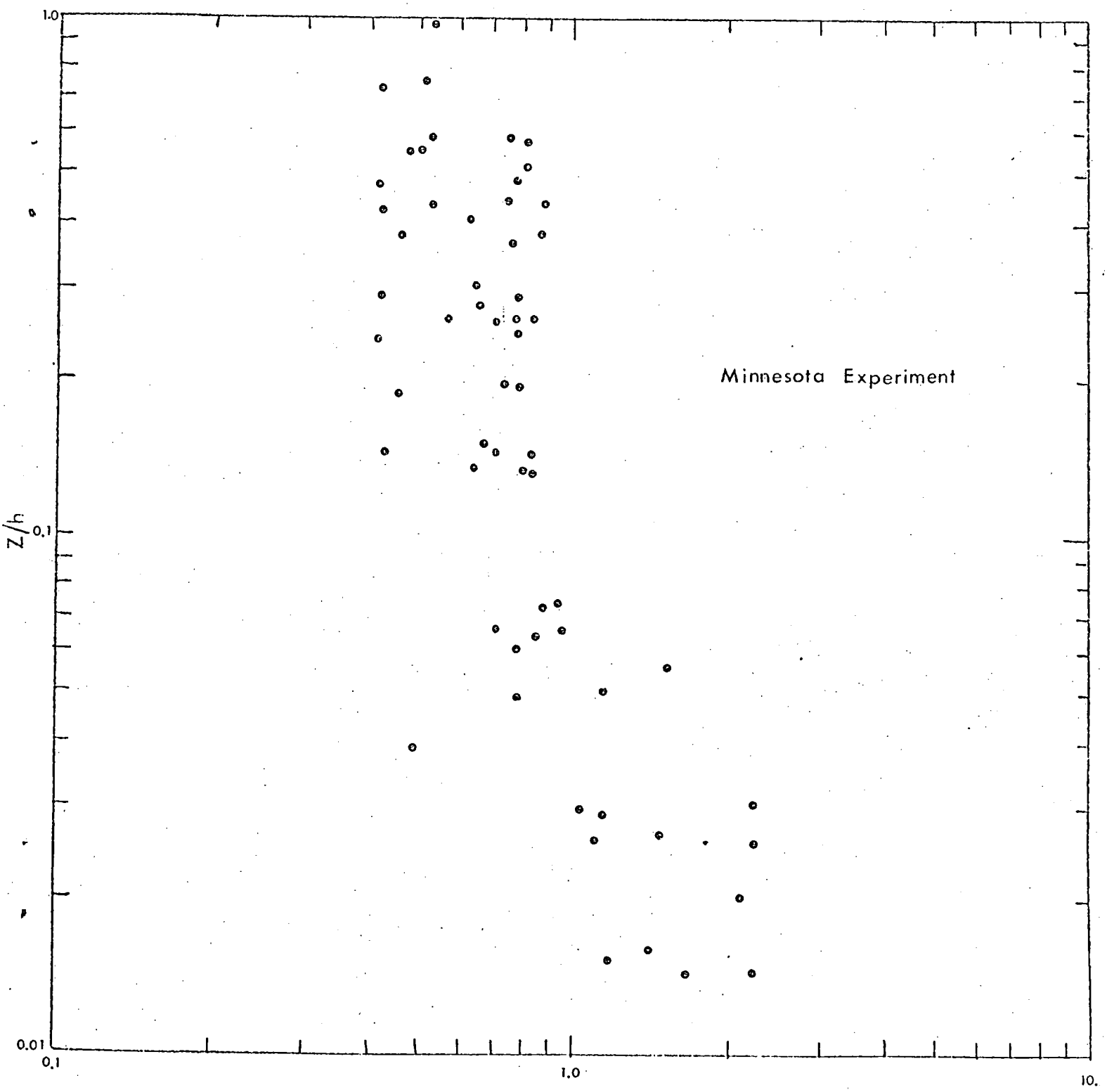
1.0
0.1
0.01
Z/h
0.1
1.0
10.
Minnesota Experiment
$\epsilon \Big/ \left(\frac{g}{T} Q_0\right)$

Figure 3

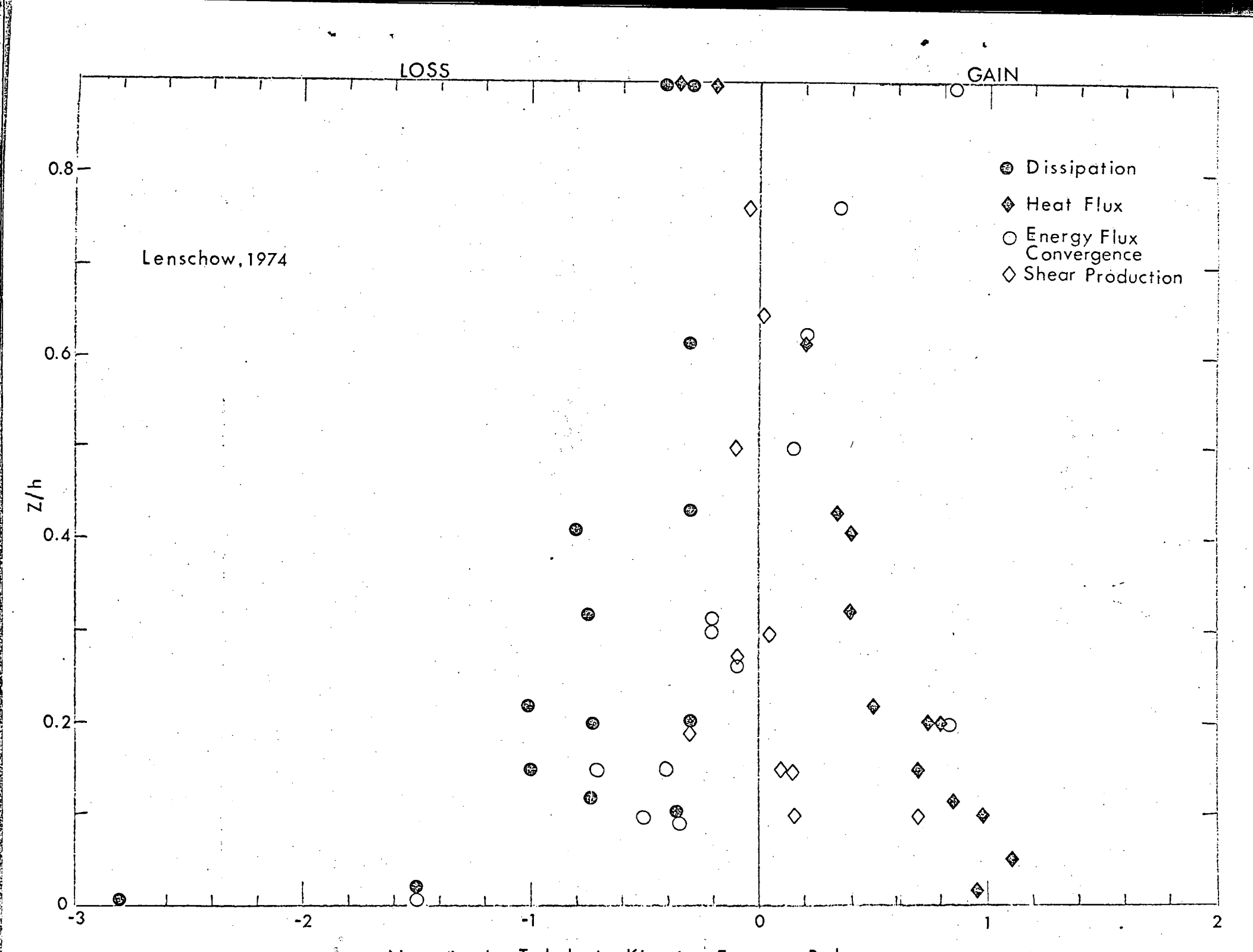
LOSS
GAIN
Dissipation
Heat Flux
Energy Flux Convergence
Shear Production
Lenschow, 1974
Z/h
0
0.2
0.4
0.6
0.8
-3
-2
-1
0
1
2
Normalized Turbulent Kinetic Energy Balance

Figure 4

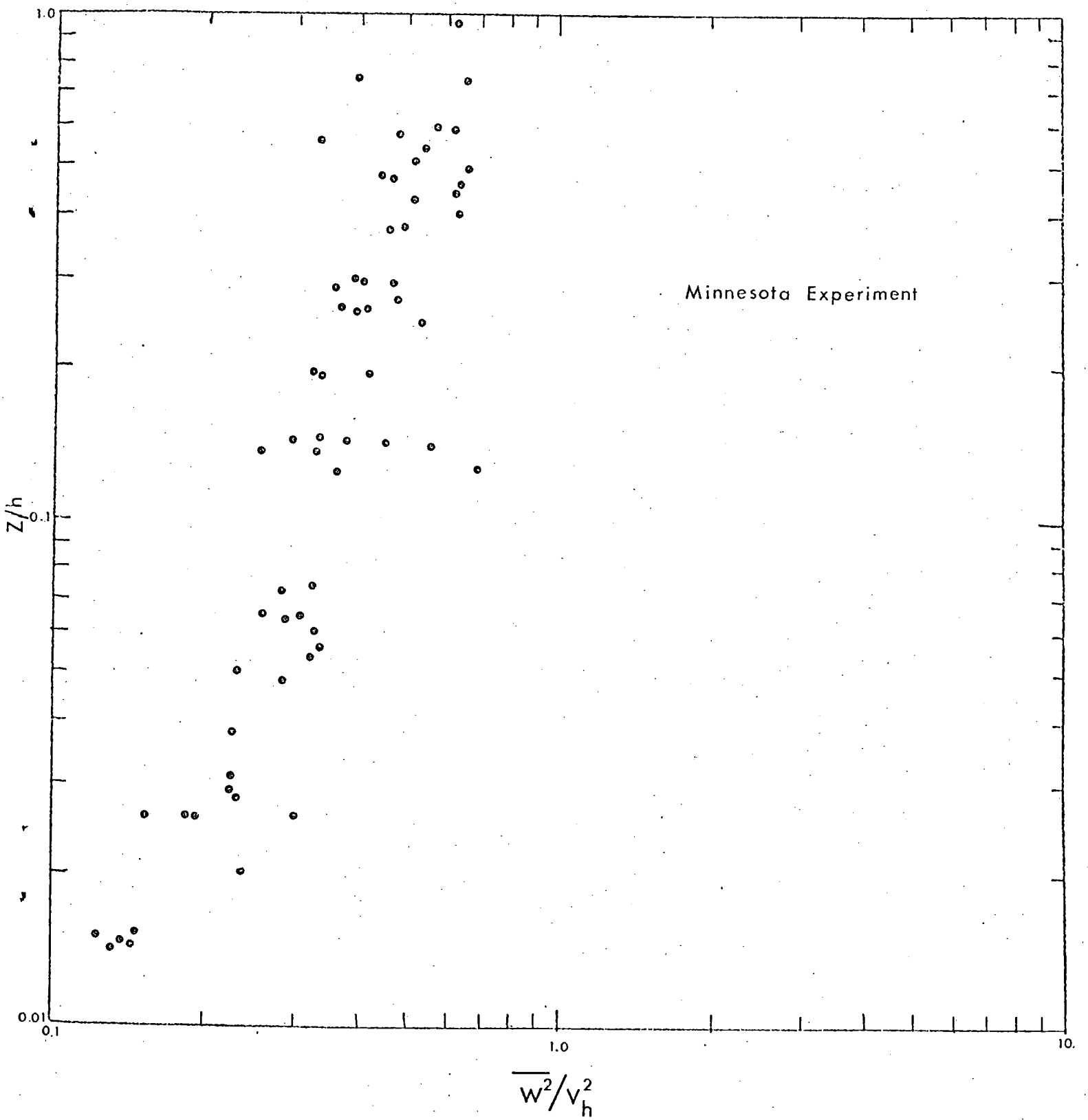

Figure 5

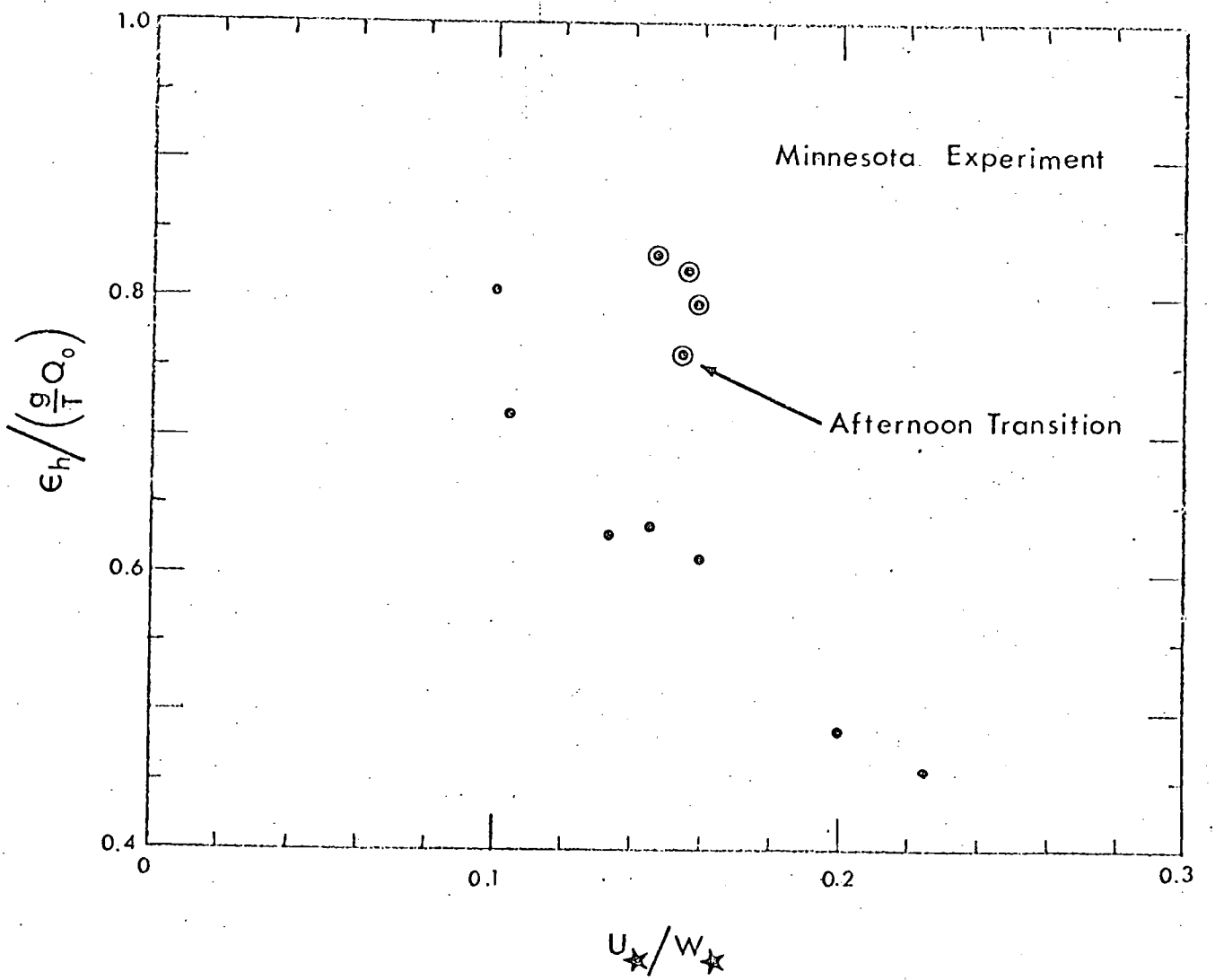
1.0
0.8
0.6
0.4
0
0.1
0.2
0.3
Minnesota Experiment
Afternoon Transition
$\epsilon_h / \left(\frac{g}{T} Q_o\right)$
U_* / W_*

Figure 6

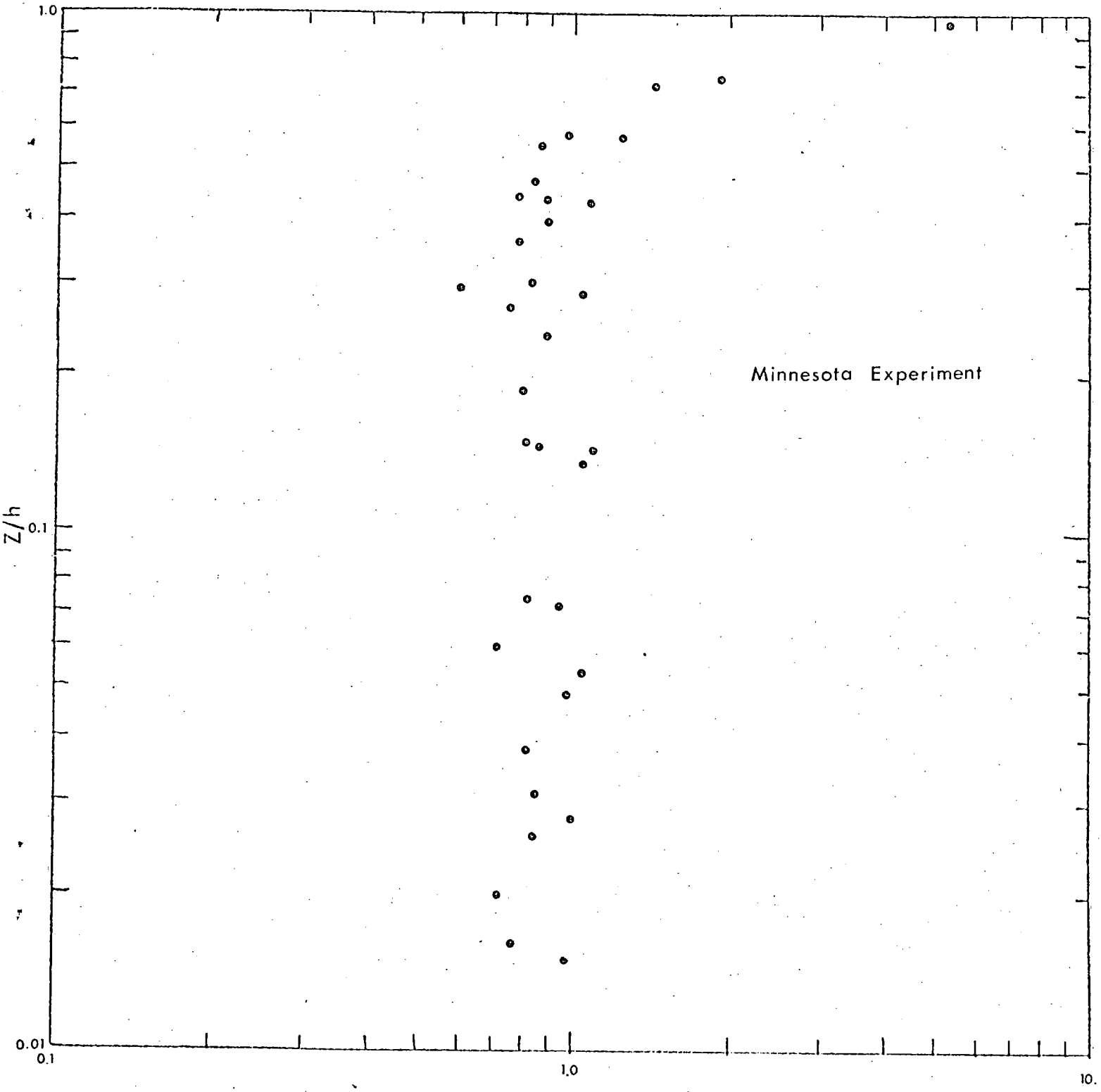

$$\frac{C_T^2}{\beta}\left(\frac{g}{T}\right)^{2/3} Q_0^{-4/3} Z^{4/3}$$

Figure 7

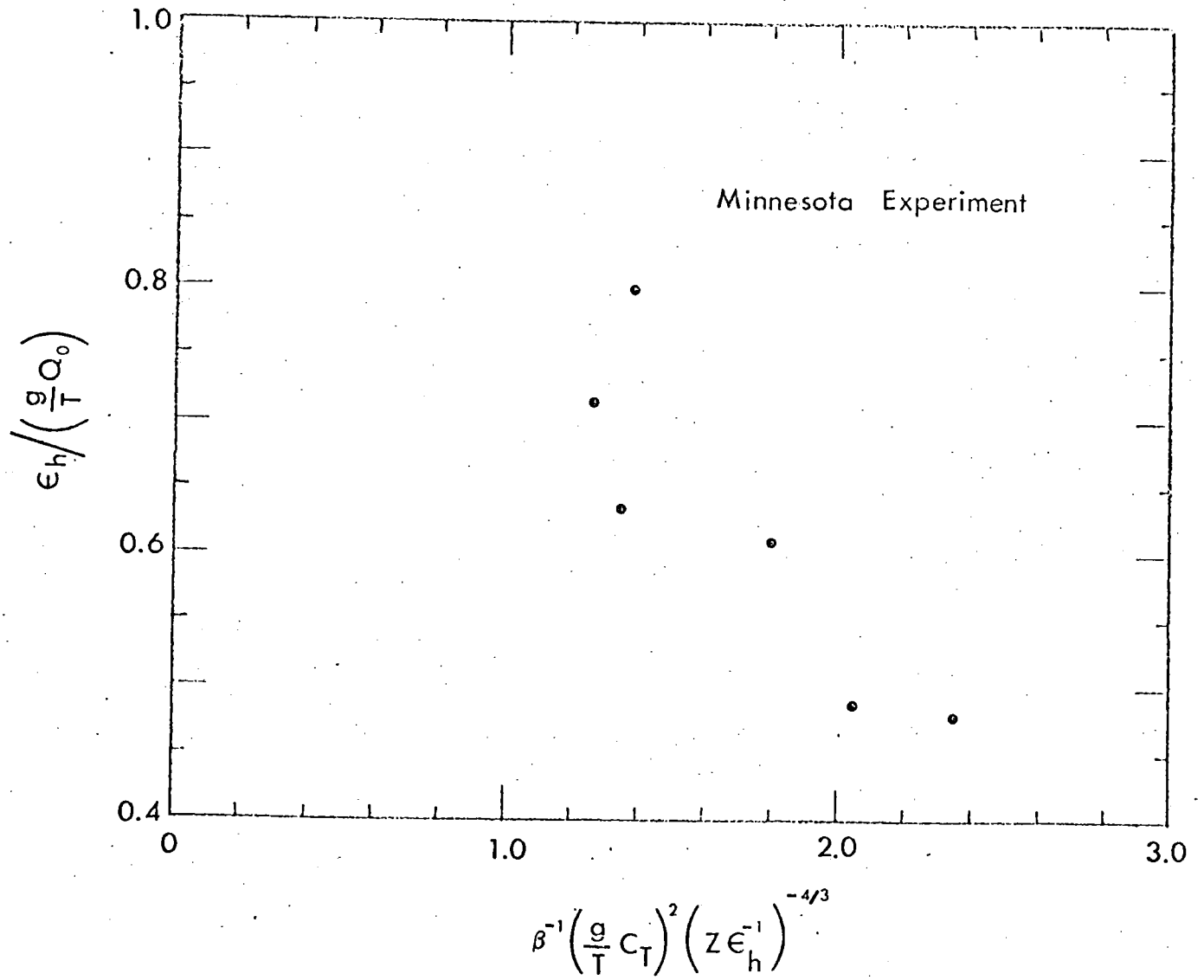
Minnesota Experiment
1.0
0.8
0.6
0.4
0
1.0
2.0
3.0
$\epsilon_h / \left(\frac{g}{T} Q_o\right)$
$\beta^{-1}\left(\frac{g}{T} C_T\right)^2 \left(Z \epsilon_h^{-1}\right)^{-4/3}$

Figure 8

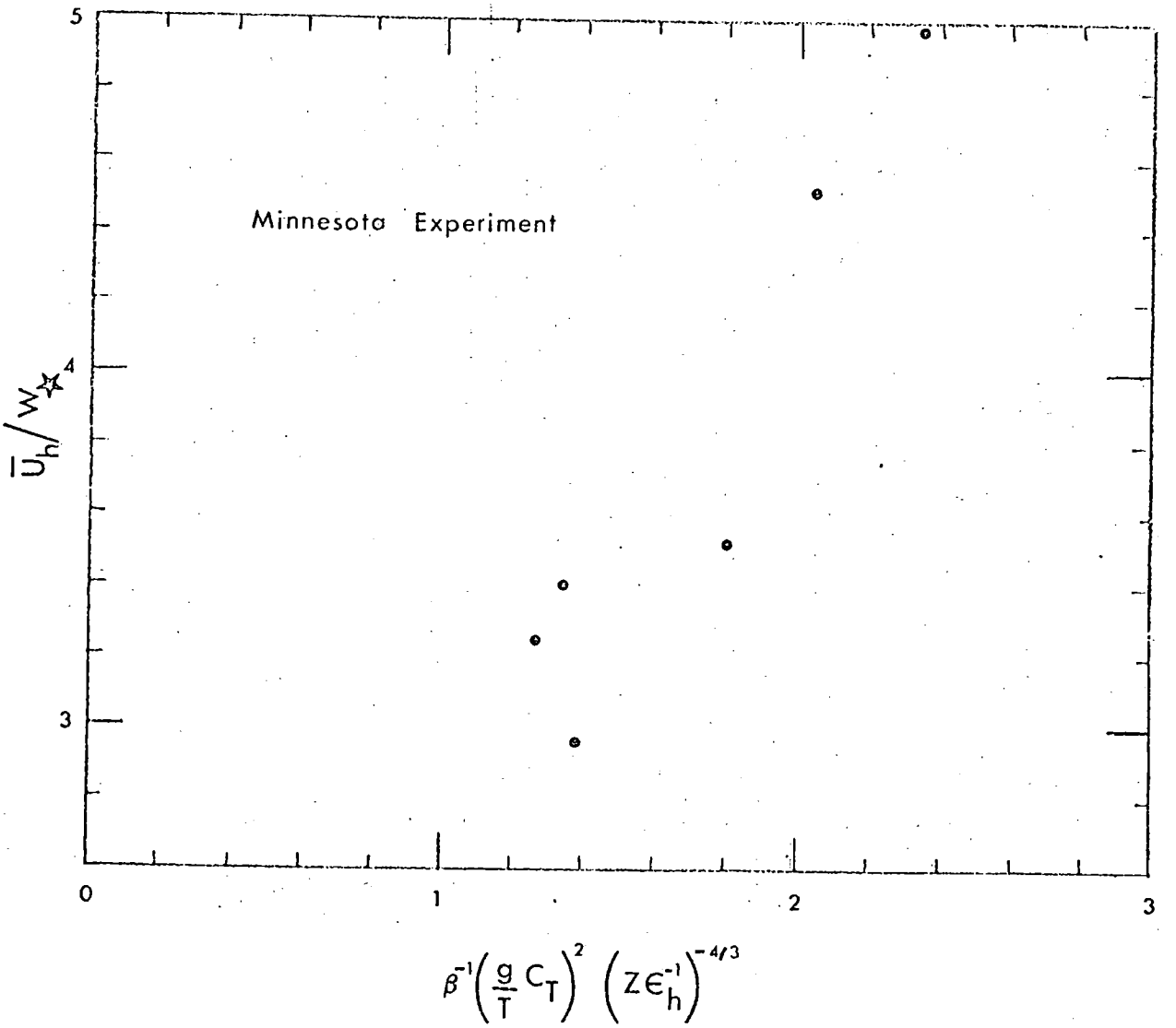
Minnesota Experiment
$\overline{U_h}/w_*$
5
4
3
0
1
2
3
$\beta^{-1}\left(\frac{g}{T}C_T\right)^2\left(z\epsilon_h^{-1}\right)^{-4/3}$

Figure 9

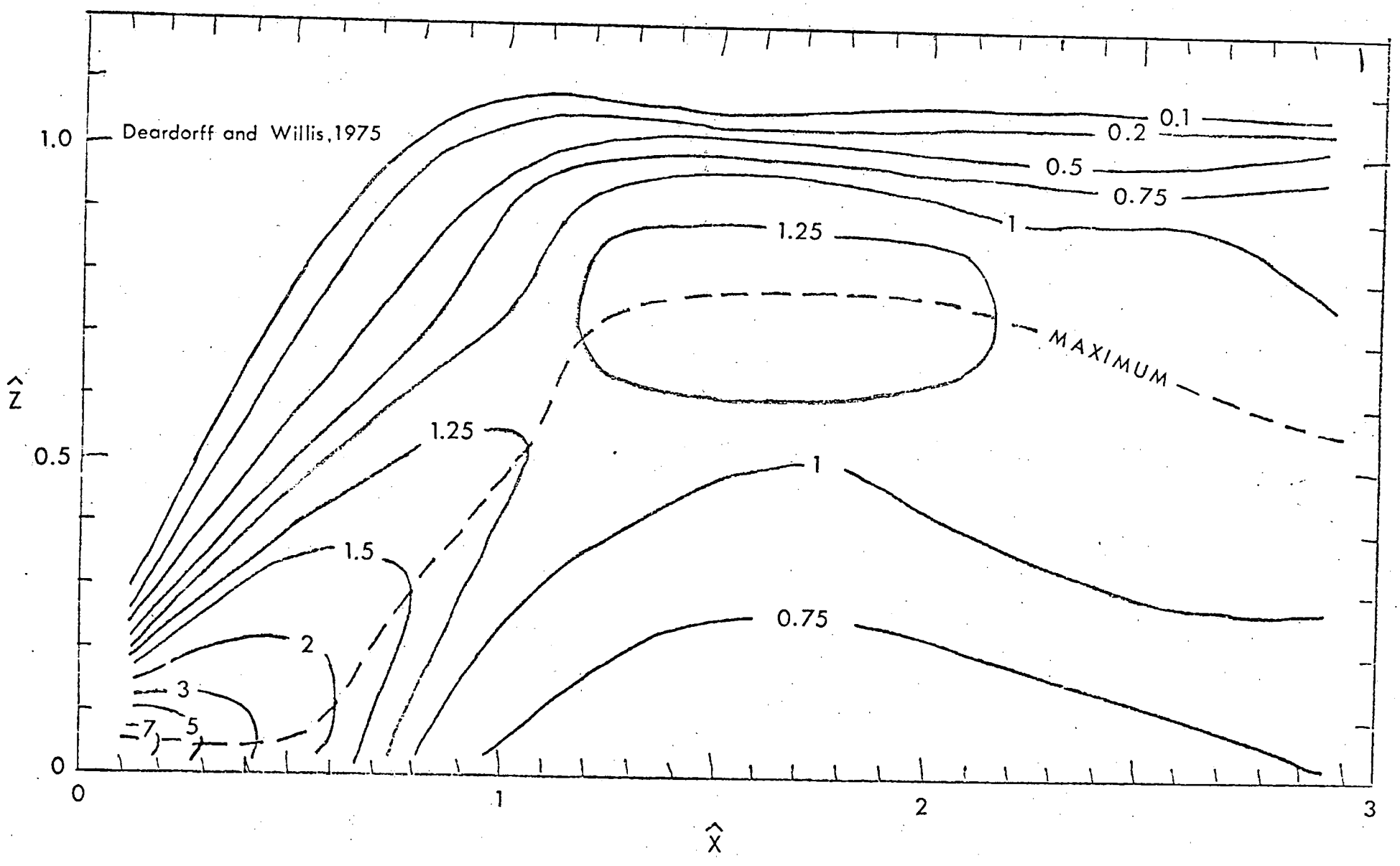
Deardorff and Willis, 1975
1.0
0.5
0
0
1
2
3
$\hat{Z}$
$\hat{X}$
0.1
0.2
0.5
0.75
1
1.25
MAXIMUM
1.25
1
1.5
0.75
2
3
5
7

Figure 10

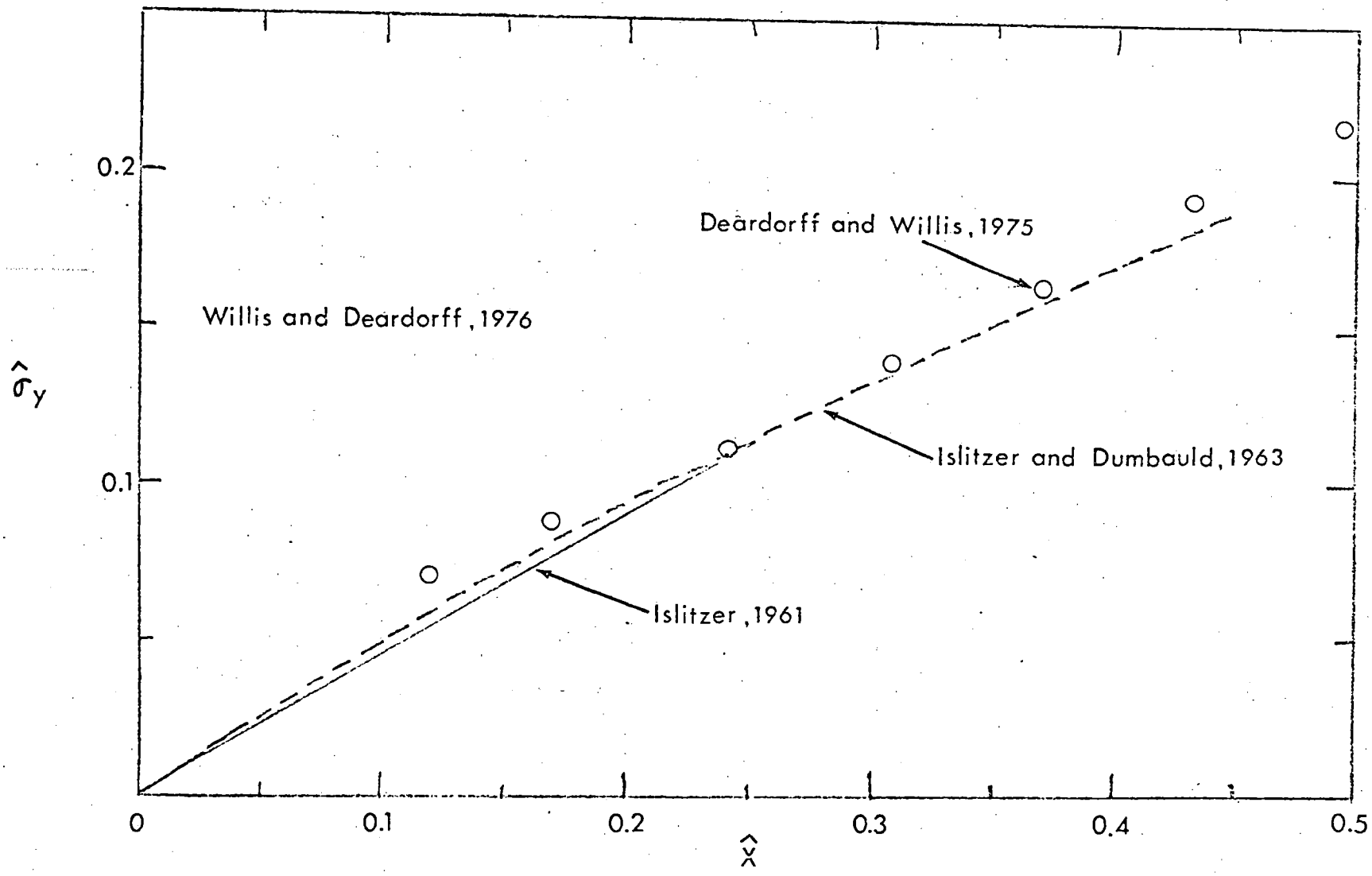
0.2
0.1
$\hat{\sigma}_y$
Deardorff and Willis, 1975
Willis and Deardorff, 1976
Islitzer and Dumbauld, 1963
Islitzer, 1961
0
0.1
0.2
0.3
0.4
0.5
$\hat{x}$

Figure 11

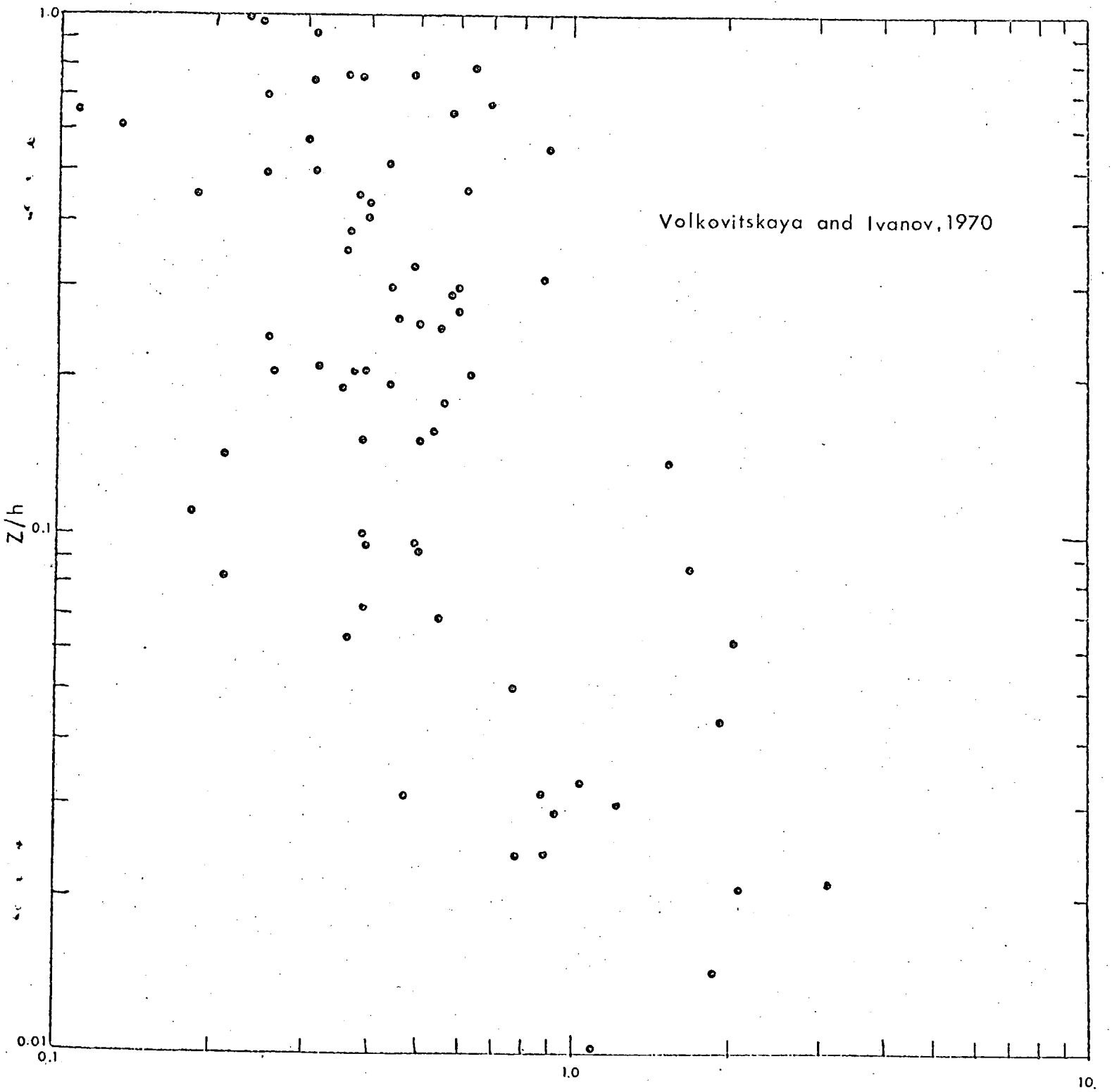
Volkovitskaya and Ivanov, 1970
Z/h
1.0
0.1
0.01
0.1
1.0
10.
$\epsilon / \left(\frac{g}{T} Q_0 \right)$

Figure 12

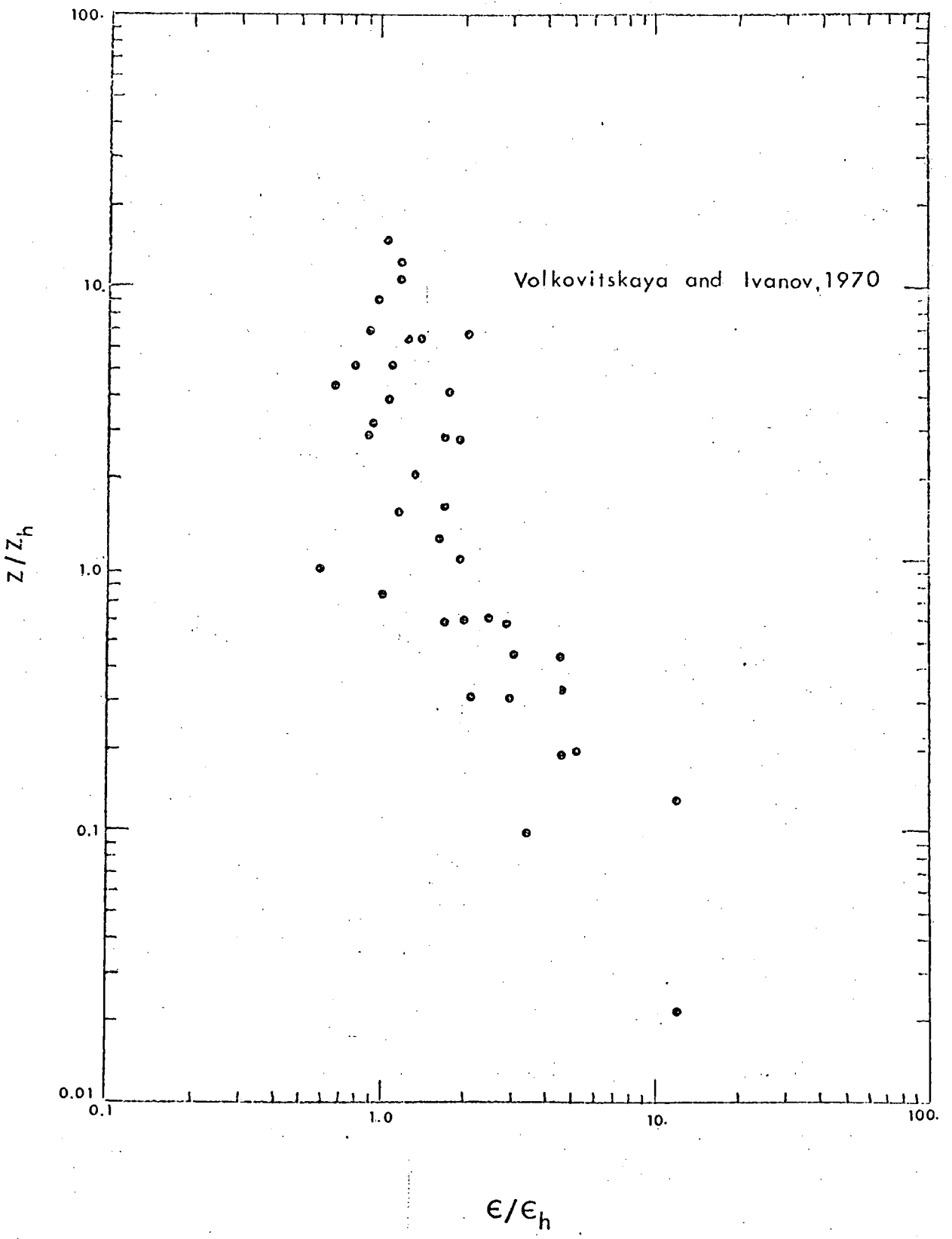
Volkovitskaya and Ivanov, 1970
100.
10.
1.0
0.1
0.01
0.1
1.0
10.
100.
Z / Z_h
ϵ/ϵ_h

Figure 13

Date Due			

BRODART, INC. Cat. No. 23 233 Printed in U.S.A.